

7.1 Introduction

Heavy metal pollution of water is one of the serious problems of the day. The major sources of heavy metals in aquatic systems are industrial discharges of industries that release heavy metals into environment. Being recalcitrant and persistent in nature, these metallic species tend to accumulate in living organisms and pose serious life-threatening hazards [Fu and Wang, 2011]. Amid various heavy metals that are toxic, chromium has widespread applications in various industries [Othman et al., 2012; Anirudhan et al., 2013]. Above the permissible limit, Cr(VI) is reported to affect human physiology and cause serious health complications extending from skin inflictions to lung cancer [Khezami and Capart, 2005]. Many methods namely membrane filtration, chemical precipitation, ion-exchange, electro-chemical techniques, adsorption, etc. have been reported for the treatment of heavy metal bearing water [Ku and Jung, 2001; Kang et al., 2004; Wang et al., 2007; El Samrani et al., 2008]. Adsorption of metallic species onto certain adsorbents is considered one of the most useful techniques offering numerous advantages such as ease in operation, simple design, low operational and maintenance cost [Volesky, 2004; Ozcan and Ozcan, 2013; Kamari et al., 2009].

This chapter deals with the investigation of cupric oxide nanoparticles for removal of Cr(VI) from aqueous solutions. The adsorption process was modelled to Box-Behnken design of response surface methodology and various experimental parameters were

optimized. The adsorption isotherm, kinetic and thermodynamic parameters were determined. In addition, linear and non-linear analyses of isotherm and kinetic parameters were carried out for achieving the best fit values of the parameters.

7.2 Results and Discussion

7.2.1 Characterization of nano-cupric oxide after adsorption of chromium

The detailed study on the structural and topographical characterization of nano-cupric oxide before adsorption has been presented elsewhere (Section 4.3.3 of Chapter 4). The X-ray diffraction pattern of nano-cupric oxide after adsorption of chromium displayed no additional peaks suggesting structural changes did not occur during the process of adsorption of Cr(VI) by adsorption on the nanoparticles (Figure 7.1). In the same way, absence of extra peaks in FTIR after adsorption also suggested that the process of removal was physical in nature (Figure 7.2). Elemental composition of the adsorbent was also explored after adsorption through EDS and the spectrum revealed peaks of Cr along with the peaks of Cu and O that confirmed its adherence on the surface (Figure 7.3).

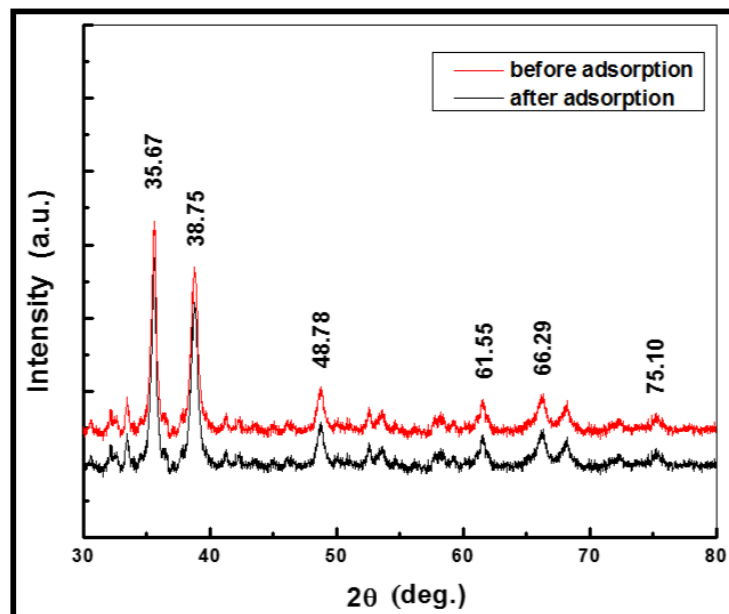


Figure 7.1 XRD pattern of nano-cupric oxide before and after adsorption of Cr(VI) ions

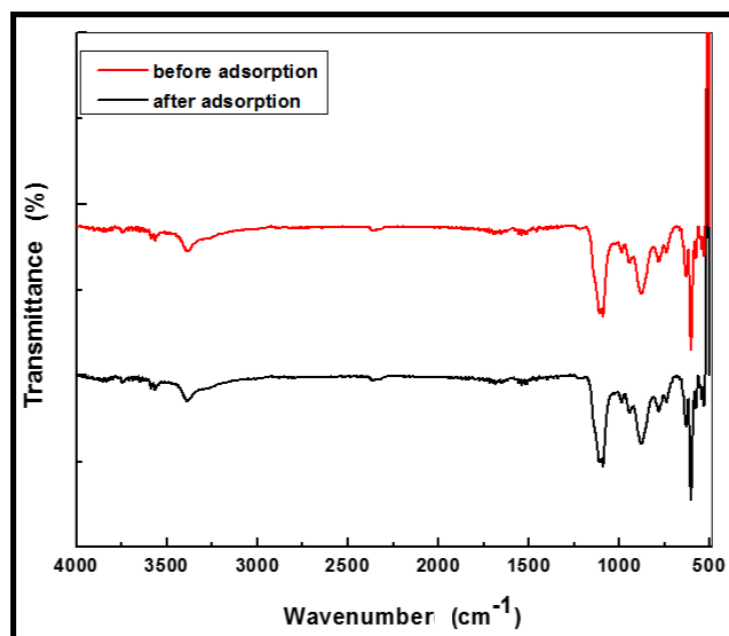


Figure 7.2 FT-IR spectrum of nano-cupric oxide before and after adsorption of Cr(VI) ions

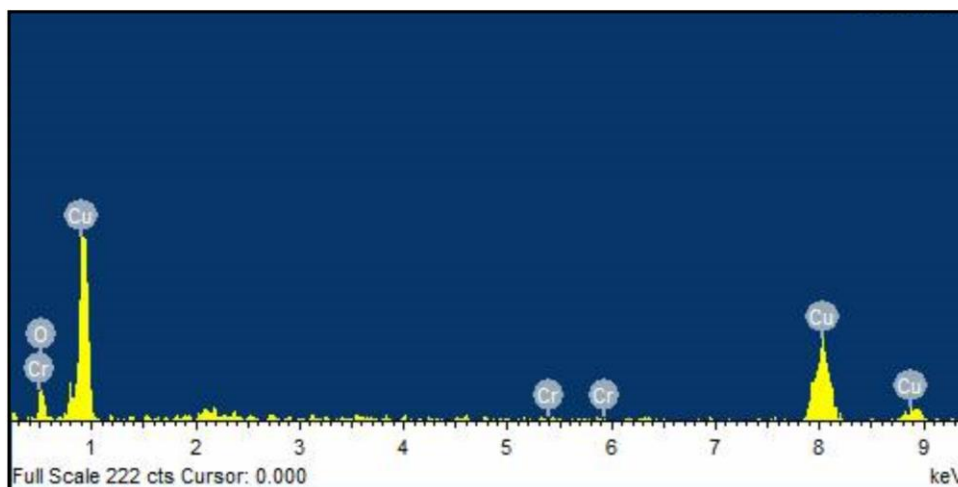


Figure 7.3 EDS pattern of nano-cupric oxide after adsorption

7.2.2 Adsorption Experiments

The experiments were conducted in batch mode for the adsorption of Cr(VI) ions on nano-cupric oxide.

7.2.2.1 Effect of experimental parameters on the removal of chromium from aqueous solutions on nano-cupric oxide

The influence of various experimental parameters on the removal of chromium was explored and the results of preliminary experiments exhibited that acidic conditions favoured the adsorption while increasing pH minified the percentage removal. The removal of Cr(VI) by nano-cupric oxide showed significant reduction when pH of the solution was raised from 2.0 to 10.0 (Figure 7.4). The optimal removal of Cr(VI) in the present system was accomplished at pH 2.0, and thus this pH was selected for the rest of the experiments. For the effect of contact time, experiments were conducted with 10

mg/L of chromium solution at different intervals and it was observed from the Figure 7.5 that the removal of metal ion increases in the beginning and after 45 min, the adsorption rate become almost steady and finally equilibrium was achieved in 45 min. Thereafter, no significant change occurred in the removal of metal ions. Removal (%) of chromium get enhanced with increased dosage of adsorbent keeping other experimental conditions fixed (Figure 7.6). The percentage removal decreased on increasing concentration from 5 mg/L to 25 mg/L due to high ratio between free sites on the adsorbent surface and metal ions in solution. Thus, the removal percentage is higher for lower concentration and vice versa as depicted in Figure 7.7.

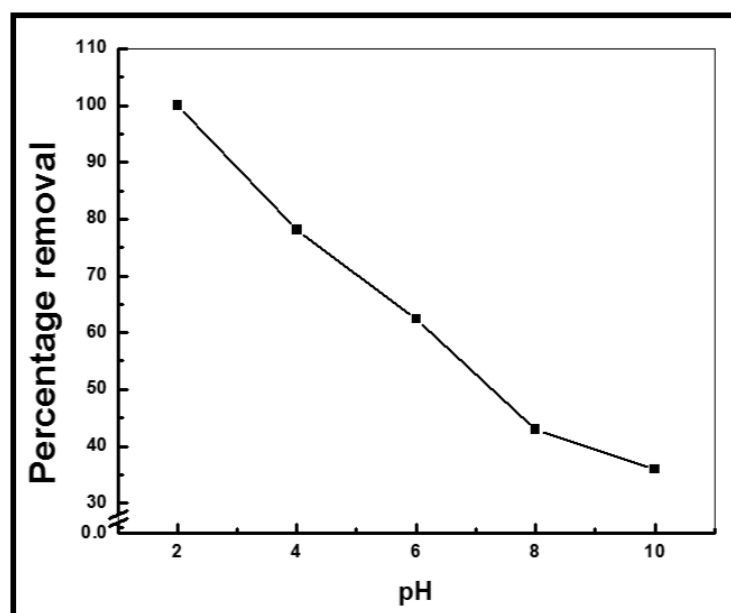


Figure 7.4 Effect of initial pH on removal (%) of chromium from aqueous solutions on nano-cupric oxide (Initial concentration= 10 mg/L, adsorbent dose= 8g/L, Temperature= 303K)

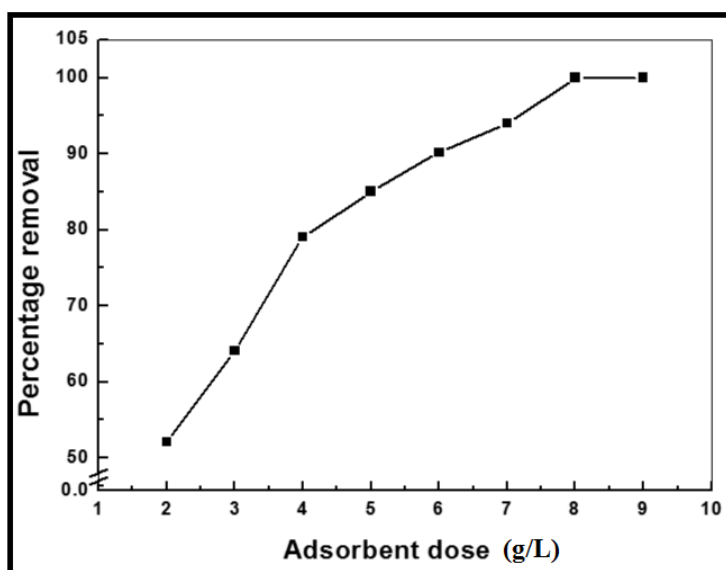


Figure 7.5 Effect of adsorbent dose on removal (%) of chromium from aqueous solution on nano-cupric oxide (Initial pH=2.0, Initial concentration =10mg/L, Temperature=303K)

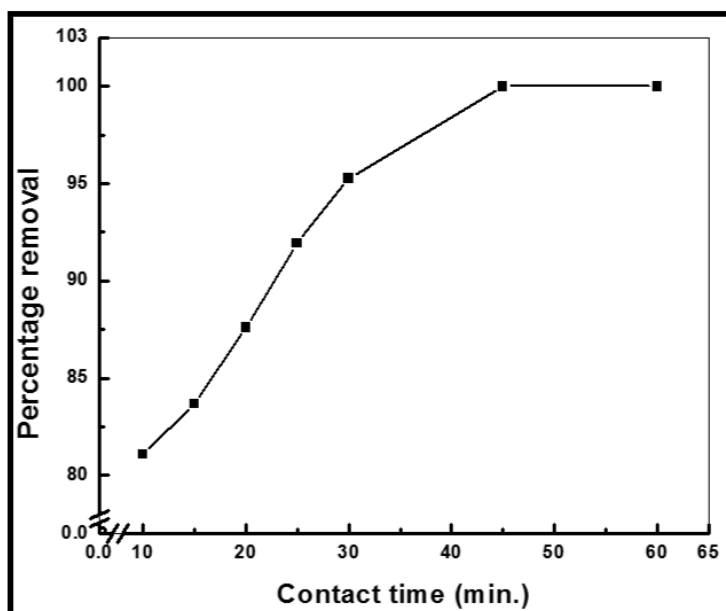


Figure 7.6 Effect of contact time on removal (%) of chromium from aqueous solutions on nano-cupric oxide (Initial concentration=10mg/L, Initial pH =2.0, Initial dose=8g/L, Temperature= 303K)

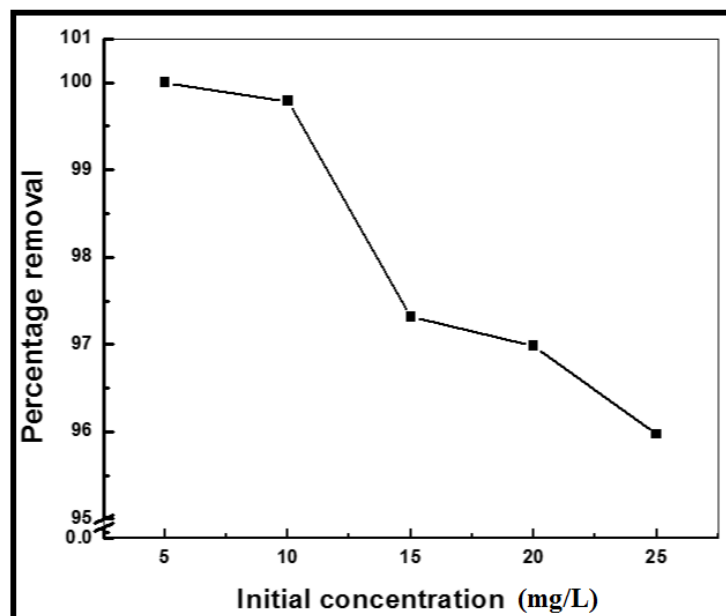


Figure 7.7 Effect of initial concentration on removal (%) of chromium from aqueous solutions on nano-cupric oxide (Initial pH= 2.0, Initial dose=8g/L, Temperature=303 K)

7.2.2.2 Design of experiment and data analysis for adsorption of chromium (VI) on nano-cupric oxide

The adsorption experiments were conducted based on the design matrix of Box-Behnken design of RSM for obtaining the response corresponding to the independent variables addressed in the experimental design matrix by applying quadratic model and corresponding results obtained have been presented in Table 7.1.

Table 7.1 Box-Behnken designed experimental runs for removal of chromium on nano-cupric oxide

Run Order	Concentration (mg/L)	pH	Dose (g/L)	Percent removal
1	5	2	11	95
2	25	2	11	99.5
3	5	10	11	82
4	25	10	11	50.4
5	5	6	2	69
6	25	6	2	76
7	5	6	20	86
8	25	6	20	81
9	15	2	2	58
10	15	10	2	80
11	15	2	20	94
12	15	10	20	93
13	15	6	11	68
14	15	6	11	68
15	15	6	11	68

The empirical relationship between the response and the independent variables namely initial concentration, pH and adsorbent dose in the coded units is presented in the form of following polynomial regression equation for removal (%) of chromium designated by Y:

$$Y = 90.63 - 2.7 (\text{concentration}) - 17.4 (\text{pH}) + 7.84 (\text{adsorbent dose}) + 7.2 (\text{concentration})^2 - 16.3 (\text{pH})^2 - 4.7 (\text{adsorbent dose})^2 - 5.2 (\text{concentration} \times \text{pH}) - 1.5 (\text{concentration} \times \text{adsorbent dose}) + 3.9 (\text{pH} \times \text{adsorbent dose}). \quad (7.1)$$

All the significant as well as insignificant terms have been included in the given regression equation for maintaining the hierarchical nature of the selected model [Dahlan et al., 2008]. In the quadratic equation (Equation 7.1), the magnitude of the coefficient represents the intensity while the sign before coefficient designates nature of influence (positive or negative) of the particular variable on the response. A positive sign of a factor means that the response is promoted when the factor level amplifies and a negative effect of the factor revealed that the response is intimidated with the escalation in factor level. Upon regression analysis, the regression equation for removal of chromium by nano-cupric oxide yielded regression coefficient $R^2 = 99.52$, higher than the $R^2 (\text{adj.}) = 97.67$. (Table 7.2) that authenticates the process of adsorption in the given range of experimental conditions.

The parameters bearing positive sign before their corresponding coefficients are inclined to increase the chromium removal (%) and vice versa [Sarkar and Majumdar, 2011]. From the equation, it has been deciphered that pH is the most dominating parameter having positive sign before its coefficient followed by adsorbent dose and concentration. Positive sign before coefficients of adsorbent dose suggested the increment in chromium removal (%) with increase in dose.

Table 7.2 Estimated regression coefficients for removal of chromium on nano-cupric oxide

Term	Coef	SE Coef	T	P
Constant	90.63	1.1946	75.869	0
Concentration	2.693	0.7315	3.681	0.014
pH	-17.357	0.7315	23.728	0
Dose	7.835	0.7315	10.711	0
Concentration*Concentration	7.221	1.0768	6.706	0.001
pH*pH	-16.319	1.0768	-15.155	0
Dose*Dose	-4.659	1.0768	-4.327	0.008
Concentration*pH	-5.162	1.0345	-4.99	0.004
Concentration*Dose	-1.463	1.0345	-1.414	0.217
pH*Dose	3.997	1.0345	3.864	0.012
S = 2.06903		PRESS = 332.571		
R-Sq = 99.52%		R-Sq(pred) = 92.56%		R-Sq(adj) = 98.66%

7.2.2.3 Analysis of variance (ANOVA)

The effectiveness of the model was investigated by applying analysis of variance (ANOVA) and the results were presented in Table 7.3. In the present case, ANOVA study

exhibited that the regression model is significant as large F-value and a low P value [Jain et al., 2011]. Among linear effect, pH was found to be the dominant parameter among other having sum of squares (Seq SS) value of 2410.26 followed by adsorbent dose and concentration.

Table 7.3 Analysis of variance for removal of chromium on nano-cupric oxide

Source	DF	Seq SS	Adj SS	Adj MS	F	P
Regression	9	4448.58	4448.58	494.29	115.46	0
Linear	3	2959.36	2959.36	986.45	230.43	0
Concentration	1	58	58	58	13.55	0.14
pH	1	2410.26	2410.26	2410.26	563.03	0
Dose	1	491.1	491.1	491.1	114.72	0
Square	3	1310.15	1310.15	436.72	102.02	0
Concentration*Concentration	1	283.85	192.54	192.54	44.98	0.001
pH*pH	1	946.15	983.27	983.27	229.69	0
Dose*Dose	1	80.14	80.14	80.14	18.72	0.008
Interaction	3	179.08	179.08	59.69	13.94	0.007
Concentration*pH	1	106.61	106.61	106.61	24.9	0.004
Concentration*Dose	1	8.56	8.56	8.56	2	0.217
pH*Dose	1	63.92	63.92	63.92	14.93	0.012
Residual Error	5	21.4	21.4	4.28		
Lack-of-Fit	3	20.68	20.68	6.89	19.15	0.050
Pure Error	2	0.72	0.72	0.36		
Total	14	4469.99				

Similarly, among square effect, pH*pH was dominant and among interactive effect, concentration*pH was significant on the basis of sum of squares value.

7.2.2.4 Interaction effect of initial Cr(VI) concentration and adsorbent dose

To evaluate the combined effect of concentration and the adsorbent dosage on the removal (%) of chromium ions from the aqueous solutions, the adsorption experiments based on the matrix predicted by the selected model were conducted with the scheduled concentration and adsorbent dose. The negative sign of coefficient of concentration in the regression equation indicates dwindling percent removal with intensification in the concentration of solution (Runs “6 and 7”; Runs ‘5 and 8’). This behavior can be ascribed to the saturation of the available active sites on adsorbent surface for interaction with metal ions present in solution with increase in the concentration of solution [Sharma and Srivastava, 2010, Wang, 2011]. The graphical representation of the combined interactions of the result of experimentation has been presented in form of contour and surface plots as shown in Figure 7.8a and 7.8b. Both these contour and surface plots revealed that removal (%) of Cr(VI) decreased on increase in initial metal ion concentration and increased with the increase in adsorbent dose.

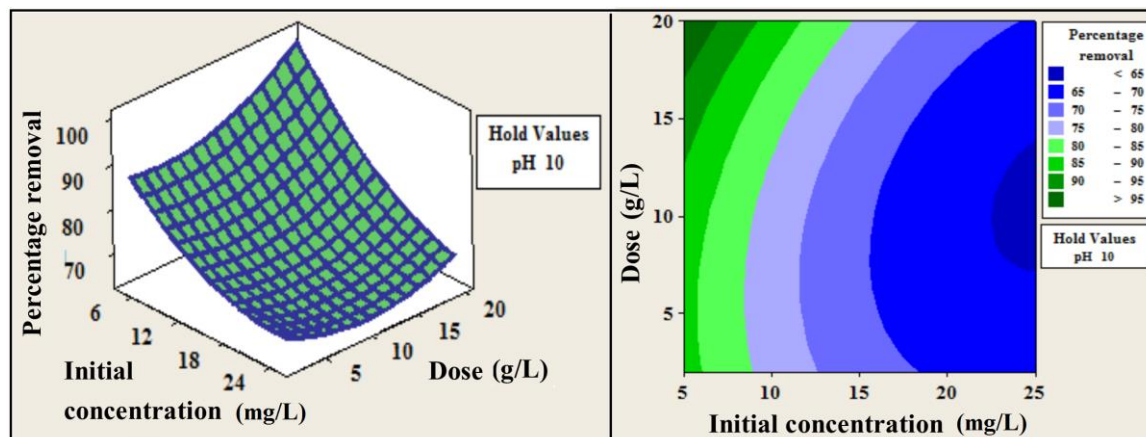


Figure 7.8 (a) Surface plot, and (b) Contour plot of percentage removal vs. dose and concentration at hold value of pH at 10

7.2.2.5 Interaction effect of pH and adsorbent dose

Perusal of literature suggested that depending on pH of the solution, different species of metal ions are present in the solution along with the adsorbate and their removal is greatly influenced by the type of their species present in the system at any particular pH.

From speciation diagram of chromium (Figure 3.1, Chapter 3), it has been found that in solution chromium exists as negatively charged ions such as HCrO_4^{2-} , CrO_4^{2-} , $\text{Cr}_2\text{O}_7^{2-}$ and $\text{Cr}_4\text{O}_{13}^{2-}$ and their existence is entirely dependent upon the pH of the solution. At lower pH, HCrO_4^{2-} is the dominant species and with a decrease in pH, the adsorbent surface tends to become more positively charged resulting in increased electrostatic interaction between negative Cr species and positive surface of adsorbent (Sharma et al., 2010).

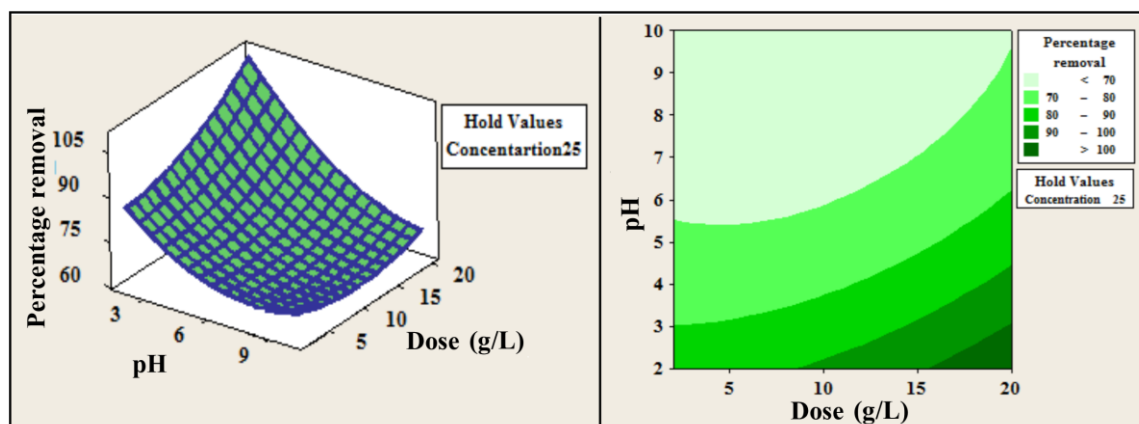


Figure 7.9. (a) Surface plot; and (b) Contour plot of percentage removal vs. pH and dose at hold value of concentration at 25 mg/L

This increased interaction lead to the increased removal of adsorbate ions from solutions with lowering of pH (Runs 1 and 5; Runs 10 and 11). In the regression equation, pH also bears a negative charge on its coefficient which indicated a remarkable decrease in the removal of adsorbate on increase in pH of the solution (Bajpai et al., 2012). Similarly, the adsorbent dose with positively charged coefficient suggested that on an increment in the dose of adsorbent, the percent (%) also increases. Increase in amount of adsorbent resulted in introduction of a number of unsaturated surface active sites. The interactive effect of both these variables upon adsorption is shown in Figures 7.9a and 7.9b. It has been observed that optimum removal is achieved at low pH (i.e. acidic condition) and high dose (Gusain et al., 2014). Conjointly, increased number of positive species and surface active sites are responsible for increased percent removal of adsorbate ions.

7.2.2.6 Interaction effect of pH and initial Cr(VI) concentration

Figure 7.10a and 7.10b displayed the interactive effect of pH and initial metal ion concentration on the percent removal of Cr(VI). It has been displayed by (Runs 8 and 11; Runs 1 and 13) that increasing initial concentration and varying pH of the solution by keeping dose at a constant value, removal percent decreases gradually. This might be due to the greater ratio of available surface for adsorbate ions at low concentrations whereas at higher concentration this ratio decreases thereby tending to decline the overall removal of adsorbate ions from solutions.

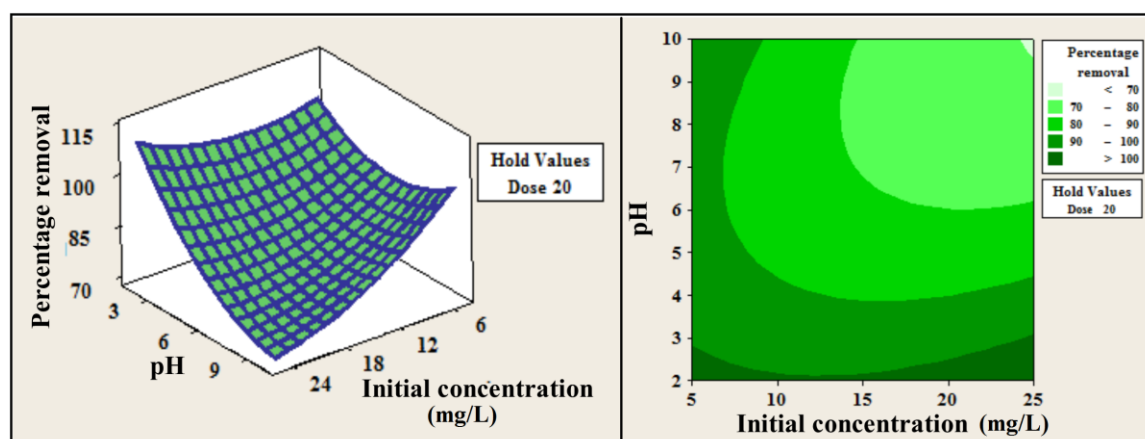


Figure 7.10 (a) Surface plot; and (b) Contour plot of percentage removal vs. pH and concentration at hold value of dose at 20 g/L

7.2.2.7 Interpretation of process optimization of removal (%) of chromium on nano-cupric oxide

The optimum value for desired response was predicted by response optimization plot (Figure 7.11). It predicted the optimum value for 100% removal of Cr(VI) from

aqueous solutions via the process of adsorption on nano-cupric oxide for the given model (pH 2.0, initial concentration 5mg/L, adsorbent dose 18.84 g/L) with the desirability score of 1. In order to verify the efficacy of model, confirmatory experiments were conducted at the predefined conditions. Further, for the confirmation experiment, dose was rounded off to 19 g/L and the experimental results were analyzed.

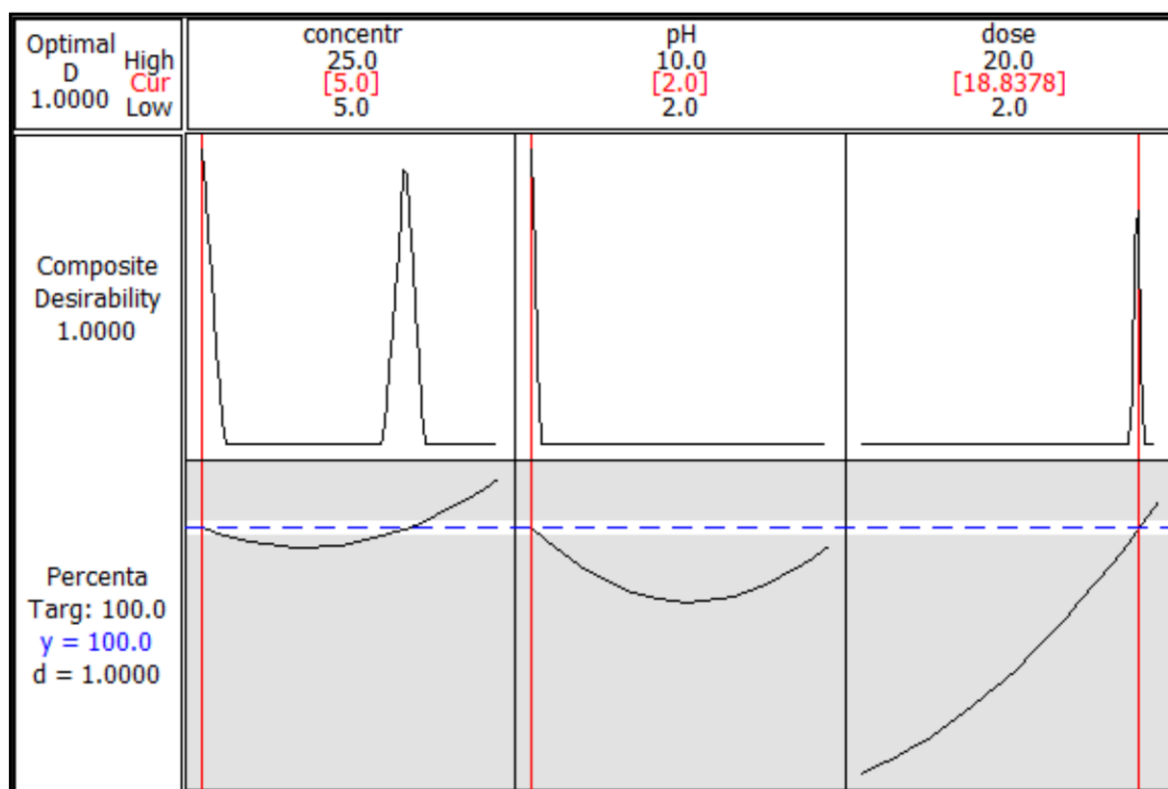


Figure 7.11. Response optimization plot for chromium removal on nano-cupric oxide

The results of confirmatory experiments exhibited that increasing concentration and pH; and decrease in dose led to decrease in removal whereas, low metal ion

concentration, low pH and higher adsorbent dosage resulted into maximum removal. However, results showed certain degree of variation than that of predicted by the model. The experimental values of the model together with the percentage error difference between the experimental and predicted value have been tabulated (Table 7.4).

Table 7.4 Confirmation experiments for removal of chromium on nano-cupric oxide

S. No.	Concentration (mg/L)	pH	Dose (g/L)	Experimental values (%)	Predicted values (%)
1	25	2.0	8.0	95.97	89.46
2	20	10	8.0	59.14	66.33
3	25	4.5	6.0	42.95	45.77
4	5	2.0	18.0	99.96	100
5	10	2.0	18.0	98.45	99.99

7.2.3 Adsorption isotherm study

In the present study, the equilibrium data incurred for Cr(VI) removal was examined with two parameters isotherm viz. Langmuir and Freundlich to ascertain the most desirable one. Additionally, linear and non-linear analysis was performed for achieving the best fit isotherm model.

The following linear and non-linear equations of Langmuir isotherm model were used [Sharma et al., 2008; Langmuir, 1916]:

$$C_e/q_e = 1/bQ^0 + C_e/Q^0 \quad (7.2)$$

$$q_e = b Q^0 C_e / (1 + b C_e) \quad (7.3)$$

where, C_e (mg/l) is the equilibrium concentration of the solute, q_e (mg/g) is amount adsorbed at equilibrium and Q^0 (mg/g) and b (L/mg) are constants related to the adsorption capacity and energy of adsorption, respectively.

Freundlich isotherm model was fitted using following linear and non-linear equations [Freundlich, 1906; Allen and McKay, 1980]:

$$\log q_e = \log K_F + 1/n \log C_e \quad (7.4)$$

$$q_e = K_F C_e^{1/n} \quad (7.5)$$

where, K_F and n are the Freundlich constants. Here, n giving a sign of how congruous the adsorption process is, and K_F ($\text{mg/g(L/mg)}^{1/n}$) represents the quantity of metal ion adsorbed on the adsorbent for a unit equilibrium concentration.

7.2.3.1 Linear analysis of adsorption isotherm

Linear analysis was carried out by fitting the equilibrium adsorption data to linear equations of Langmuir and Freundlich adsorption isotherm models. The values of theoretical maximum adsorption capacity, Q^0 (mg g^{-1}) and Langmuir adsorption constant

b ($L\ mg^{-1}$) were obtained from the slope and intercept of the plot of C_e/q_e vs. C_e , respectively (Figure 7.12) and the parameters of Freundlich isotherm model, K_F (mg/g) and n ($g\ L^{-1}$) of the adsorption were calculated from the intercept and slope of the linear plot of $\ln q_e$ vs. $\ln C_e$, respectively (Figure 7.13). Larger values of n inferred strong interaction between adsorbate and adsorbent making the adsorption process favourable [Pandey et al., 2010]. K_F value as well as n showed decline with increase in temperature affirmed the exothermic nature of removal process.

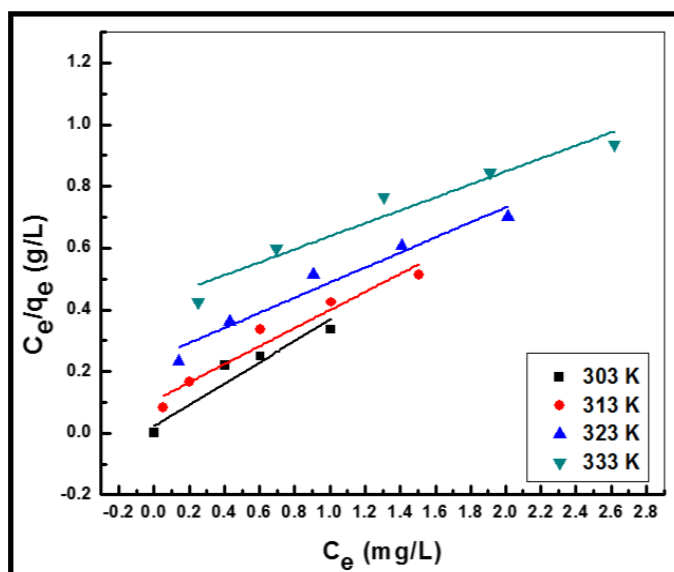


Figure 7.12 Linear Langmuir isotherm plot of chromium removal on nano-cupric oxide (symbols represent the experimental data and straight lines represent the data estimated by the model)

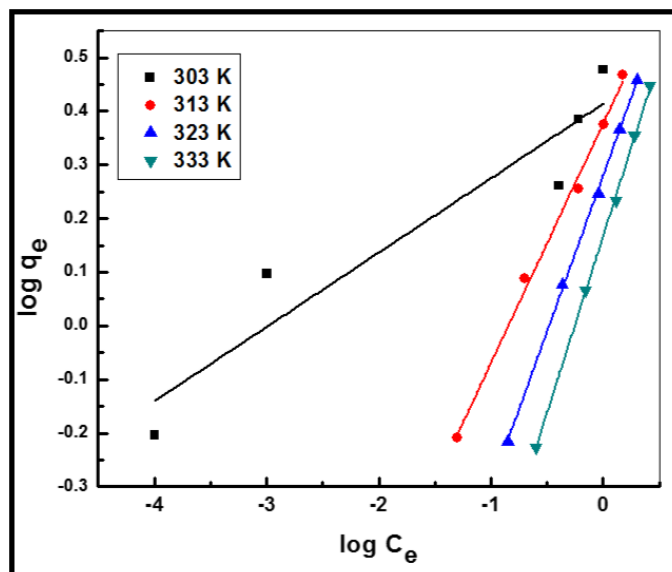


Figure 7.13 Linear Freundlich isotherm plot of chromium removal on nano-cupric oxide (symbols represent the experimental data and straight lines represent the data estimated by the model)

The isotherm parameters along with their respective correlation coefficients (R^2) obtained from the plots have been summarized in Table 7.5. The high correlation coefficient at all temperatures exhibited that Freundlich model provided the best correlation and thus is applicable for interpretation of the experimental data on the entire concentration range.

Table 7.5 Langmuir and Freundlich isotherm parameters for linear analysis for adsorption of chromium from aqueous solution on nano-cupric oxide

Analysis	Linear									
Isotherm	Langmuir Parameters					Freundlich Parameters				
Temperature (K)		303	313	323	333		303	313	323	333
Constants	Q° (mg)	4.76	4.09	3.41	2.89	K _F (mg/g (L/mg) ^{1/n})	2.59	2.38	1.90	1.47
	b (L/mg)	0.49	1.00	2.76	15.89	n	7.21	2.24	1.72	1.52
Coefficient of determination (R ²)		0.914	0.938	0.941	0.923		0.874	0.994	0.999	0.999

7.2.3.2 Non-linear analysis of adsorption isotherm

Non-linear analysis was performed by altering in-built functions namely Langmuir EXT 1, and Freundlich EXT of origin for Langmuir and Freundlich equations, respectively (Figures 7.14 and 7.15). In addition to that, customized isotherm function was also used in origin. where initial parameter was taken as numerically one. On curve fitting, both the in-built functions as well as customised user defined functions (Figures 7.16 and 7.17) depicted significant differences between the experimental data and data predicted by the models (Table 7.6 and 7.7). Thus, among linear and non-linear analyses

for isotherm parameter determination, linear was evidenced to be the more appropriate than non-linear approach having high coefficient of determination, R^2 adj. values.

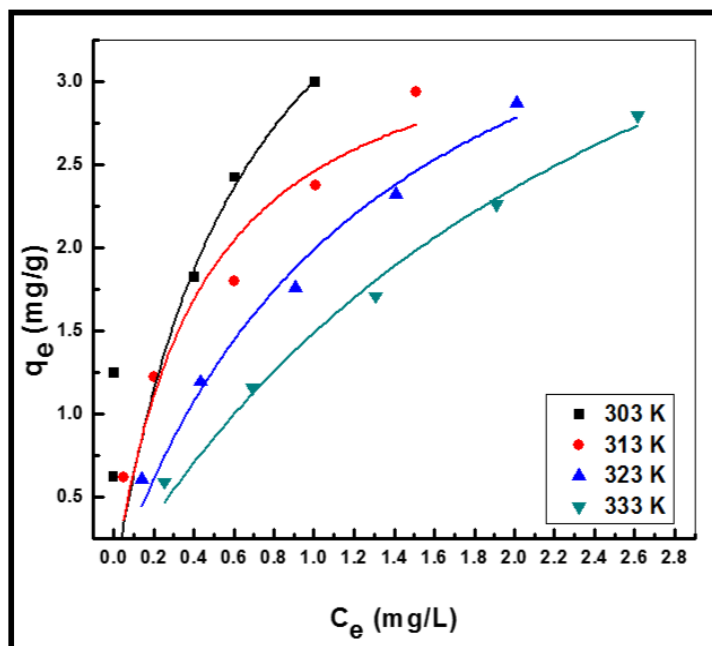


Figure 7.14 Non-linear Langmuir isotherm plot of chromium removal on nano-cupric oxide obtained by in-built Microcal origin function (symbols represent the experimental data and straight lines represent the data estimated by the model)

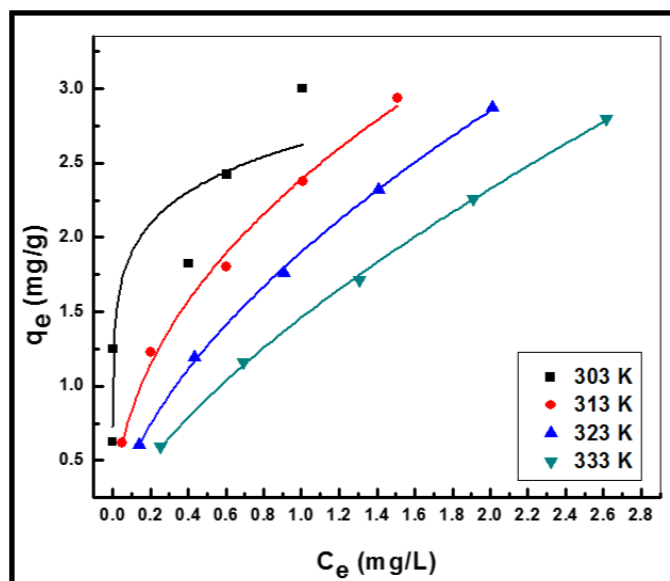


Figure 7.15 Non-linear Freundlich isotherm plot of chromium removal on nano-cupric oxide obtained by in-built Microcal origin function (symbols represent the experimental data and lines represent the data estimated by the model)

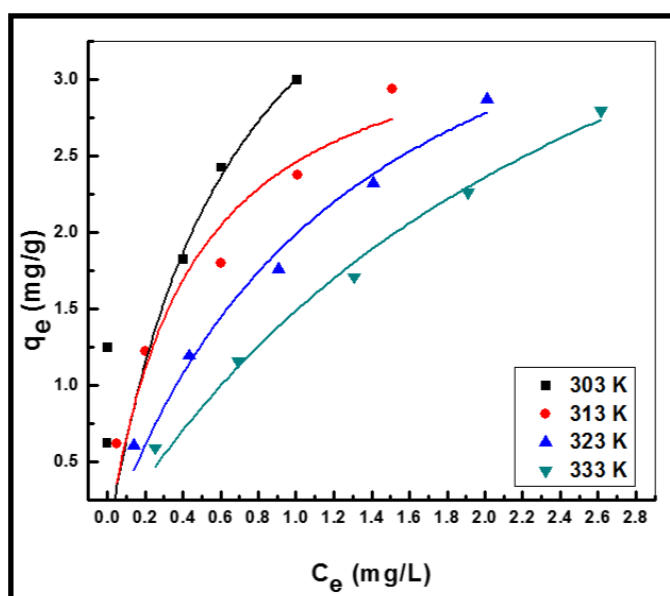


Figure 7.16 Non-linear Langmuir isotherm plot of chromium removal on nano-cupric oxide obtained by customized Microcal origin function (symbols represent the experimental data and lines represent the data estimated by the model)

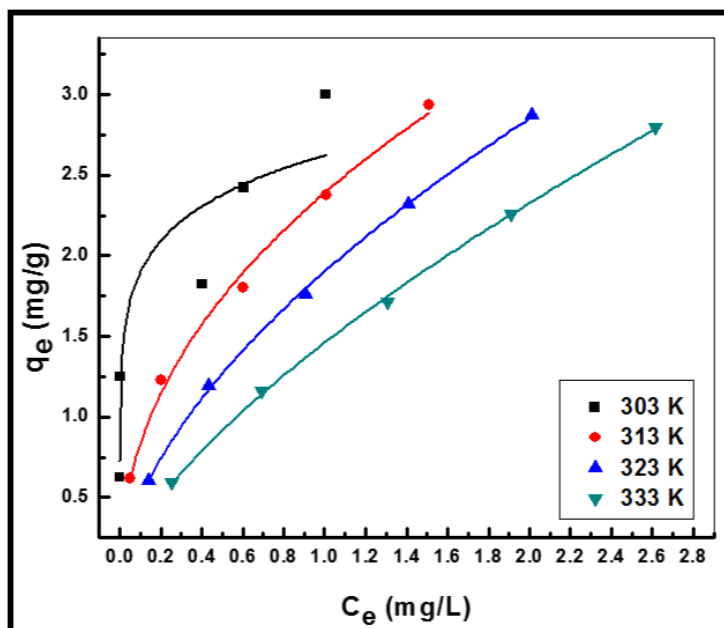


Figure 7.17 Non-linear Freundlich isotherm plot of chromium removal on nano-cupric oxide obtained by customized Microcal origin function (symbols represent the experimental data and lines represent the data estimated by the model)

Table 7.6 Langmuir and Freundlich isotherm parameters for non-linear analysis obtained by in-built Microcal origin functions for adsorption of chromium from aqueous solution on nano-cupric oxide

Analysis	Non-linear									
Isotherm	Langmuir Parameters					Freundlich Parameters				
Temperature (K)		303	313	323	333		303	313	323	333
Constants	Q^o (mg/)	5.05	3.54	4.59	5.66	K_F (mg/g (L/mg) ^{1/n})	2.62	2.39	1.90	1.46
	b (L/mg)	1.47	2.28	0.77	0.36	n	0.14	0.46	0.58	0.67
Coefficient of determination (R ²)		0.263	0.926	0.977	0.986		0.829	0.993	0.999	0.999

Table 7.7 Langmuir and Freundlich isotherm parameters for non-linear analysis obtained by customized Microcal origin functions for adsorption of chromium from aqueous solution on nano-cupric oxide

Analysis	Customized									
	Isotherm	Langmuir Parameters				Freundlich Parameters				
Temperature (K)		303	313	323	333		303	313	323	333
Constants	Q^0 (mg)	5.05	3.54	4.59	5.66	K_F (mg/g (L/mg) ^{1/n})	2.62	2.39	1.90	1.46
	b (L/mg)	1.47	2.28	0.77	0.36	n	7.17	2.19	1.71	1.49
Coefficient of determination (R^2)		0.263	0.926	0.977	0.986		0.829	0.993	0.999	0.999

7.2.4 Adsorption kinetic modeling

For rate governing step of adsorption, the mechanism of interaction of adsorbent and adsorbate and rate of metal uptake, the data was investigated by fitting the adsorption data to kinetic models, namely pseudo-first-order, pseudo-second-order and intra-particle diffusion models [Uma et al. 2013]. Moreover, linear and non-linear analysis of the adsorption data was carried out for achieving the best fit kinetic model.

The pseudo-first-order kinetic model has been widely used to predict the sorption kinetics and can be expressed by the following linear and non-linear equations [Hodaifa et al., 2013]:

$$dq/dt = k_1 (q_e - q_t) \quad (7.6)$$

$$\ln (q_e - q_t) = \ln q_e - k_1 t \quad (7.7)$$

$$q_t = q_e (1 - \exp (-k_1 t)) \quad (7.8)$$

where, $k_1(\text{min}^{-1})$ is the first order rate constant, q_e and q_t are the amount of adsorbate species adsorbed on adsorbent at equilibrium and at any time, t , respectively.

Pseudo-second order model is based on the assumption that the rate limiting step is chemi-sorption. The model is represented in the form of following linear and non-linear equations [Ho and McKay, 1998]:

$$dq/dt = k_2 (q_e - q_t)^2 \quad (7.9)$$

$$q_t = k_2 q_e^2 t / 1 + k_2 q_e t \quad (7.10)$$

where, $k_2(\text{g mg}^{-1} \text{min}^{-1})$ is the rate constant for pseudo-second-order model equation

7.2.4.1 Linear analysis of adsorption kinetics

Figure 7.18 displayed the linear analysis of kinetic data, and the kinetic parameters viz., k_1 and q_e for pseudo-first-order model, Lagergren model, were determined from the slope and intercept of the plot of $\log (q_e - q_t)$ vs. t , respectively. For, pseudo-second-order kinetic parameters, the plot of t/q_t vs. t for the model yielded a straight line from which k_2 and the equilibrium adsorption capacity (q_e) were calculated

from the intercept and slope of this line, respectively (Figure 7.19). The values of the pseudo-first-order and pseudo-second-order kinetic models along with their corresponding correlation coefficients were presented in Table 7.8. On comparing the $q_e(\text{cal.})$ values with the $q_e(\text{exp.})$ values determined by both the models, the values obtained by pseudo-second-order model were very close to $q_e(\text{exp.})$ values for all temperatures under study than pseudo-first-order model. The value of correlation coefficient (R^2) for pseudo-first-order model was also lower as compared to pseudo-second-order kinetics model. Thus, it was inferred from the value of R^2 and closeness of experimental and theoretical adsorption capacity (q_e) that pseudo-second order kinetic model better explained the experimental data on linear analysis.

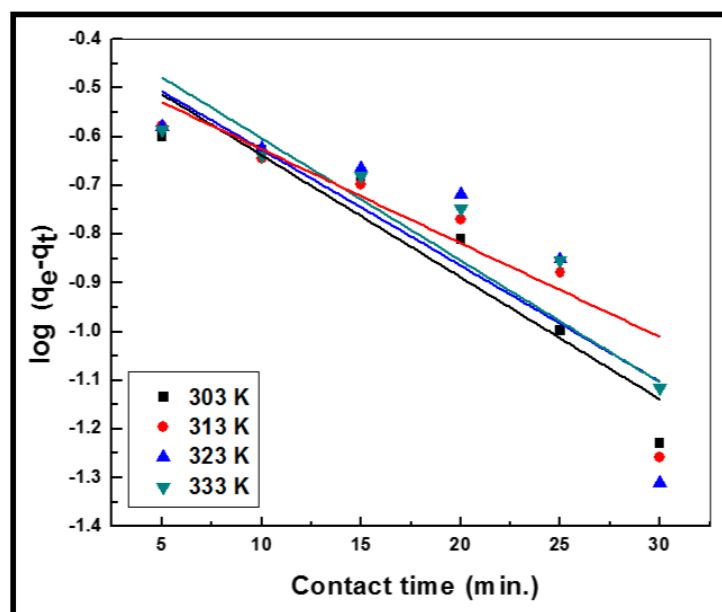


Figure 7.18 Linear pseudo-first order plot of chromium removal on nano-cupric oxide (symbols represent the experimental data and straight lines represent the data estimated by the model)

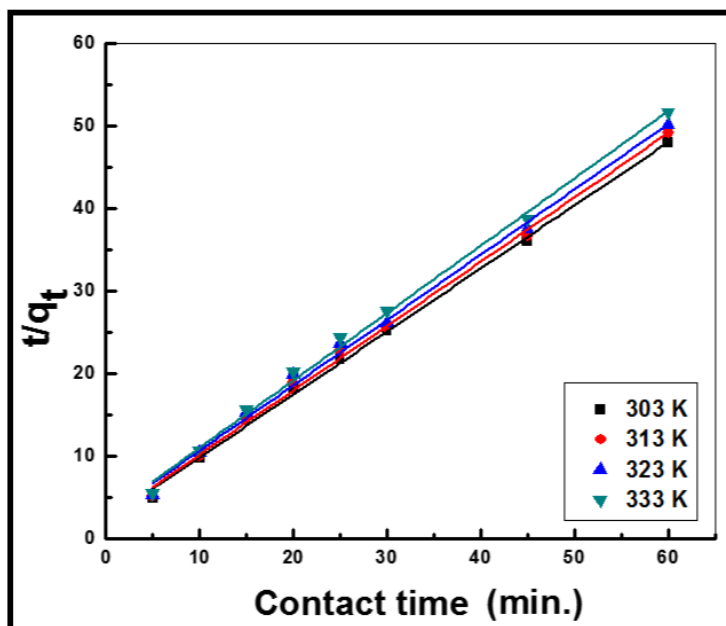


Figure 7.19 Linear pseudo-second order plot of chromium removal on nano-cupric oxide (symbols represent the experimental data and straight lines represent the data estimated by the model)

7.2.4.2 Non-linear analysis of adsorption kinetics

In-built functions of Microcal origin namely Langmuir EXT 1 and BoxLucas 1 were incorporated for non-linear analysis of adsorption data for pseudo-first order and pseudo-second order kinetic equations respectively (Figures 7.20 and 7.21). Customized user defined isotherm function was also used in which initial parameter was taken as numerically one; similar to that of the non-linear analysis of isotherm (Figures 7.22 and 7.23). From the figures, it was found that there lies a significant difference between the experimental data and data predicted by the models during non-linear analysis (Table 7.8 and 7.9).

Therefore, linear approach better explained the kinetic data than the non-linear approach having high R^2 adj. values.

Table 7.8 Pseudo-first order and pseudo-second order kinetic parameters for linear analysis and non-linear analysis by Microcal origin for adsorption of chromium from aqueous solution on nano-cupric oxide

Kinetic model	Pseudo-first order Parameter						
	Analysis	Linear			Non-linear		
Temperature (K)	q_e (exp.)	q_e (mg/g)	k_1 (1/min)	R^2 adj.	q_e (mg/g)	k_1 (1/min)	R^2 adj.
303	1.25	0.41	-0.06	0.887	1.16	0.35	0.24
313	1.22	0.41	-0.05	0.786	1.12	0.34	0.27
323	1.19	0.44	-0.06	0.687	1.09	0.33	0.19
333	1.16	0.36	-0.04	0.838	1.06	0.33	0.22
Kinetic model	Pseudo-second order Parameter						
	Analysis	Linear			Non-linear		
Temperature (K)	q_e (exp.)	q_e (mg/g)	k_2 ($\text{g}\cdot\text{mg}^{-1}\cdot\text{min}^{-1}$)	R^2 adj.	q_e (mg/g)	k_2 ($\text{g}\cdot\text{mg}^{-1}\cdot\text{min}^{-1}$)	R^2 adj.
303	1.25	1.31	0.25	0.998	1.21	0.48	0.68
313	1.22	1.28	0.24	0.997	1.18	0.46	0.61
323	1.19	1.26	0.22	0.995	1.14	0.49	0.64
333	1.16	1.23	0.22	0.996	1.24	0.49	0.68

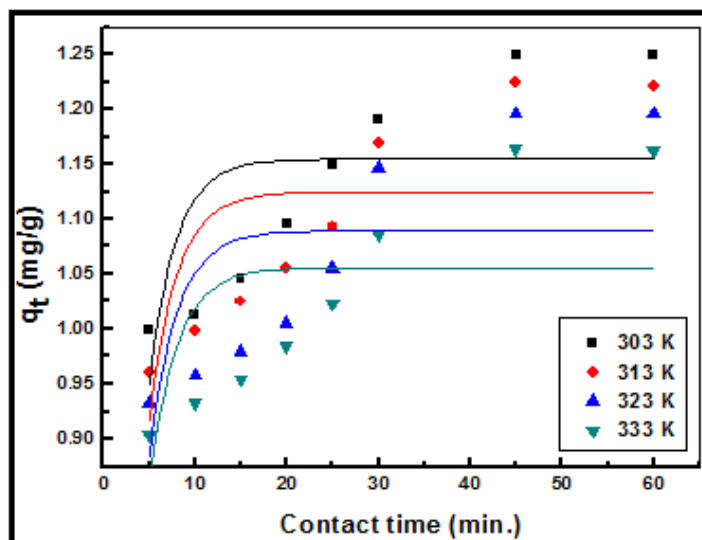


Figure 7.20 Non-linear pseudo-first order plot of chromium removal on nano-cupric oxide obtained by in-built Microcal origin function (symbols represent the experimental data and lines represent the data estimated by the model)

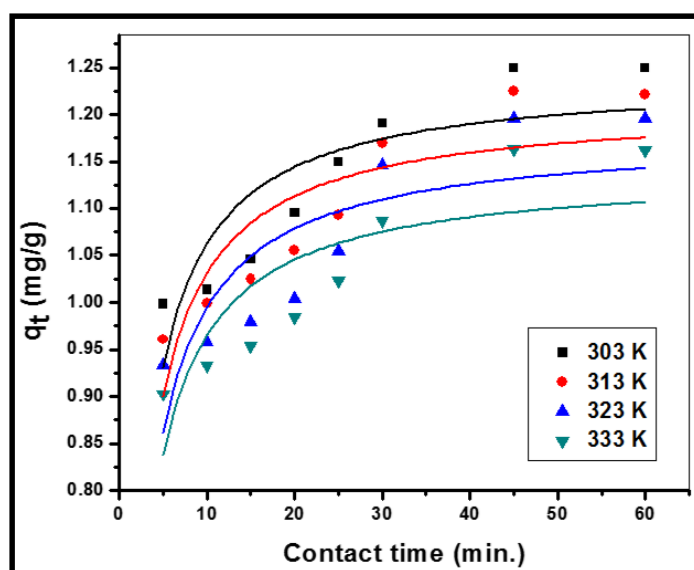


Figure 7.21 Non-linear pseudo-second order plot of chromium removal on nano-cupric oxide obtained by in-built Microcal origin function (symbols represent the experimental data and lines represent the data estimated by the model)

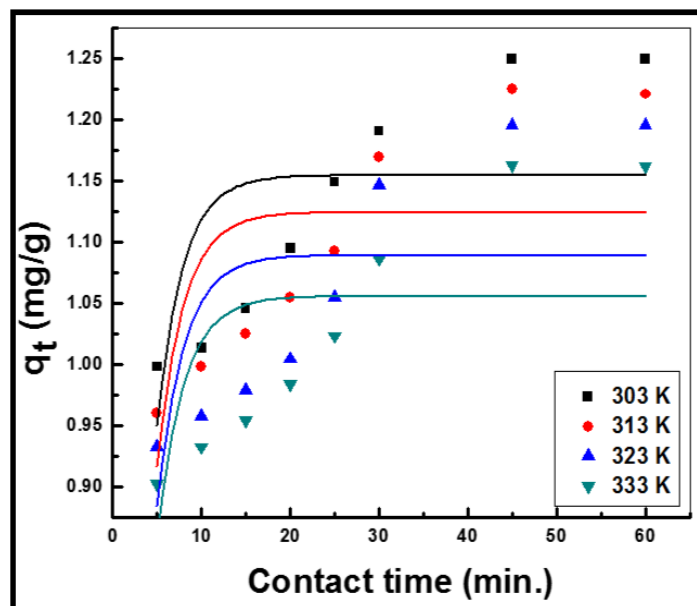


Figure 7.22 Non-linear pseudo-first order plot of chromium removal on nano-cupric oxide obtained by customized Microcal origin function (symbols represent the experimental data and lines represent the data estimated by the model)

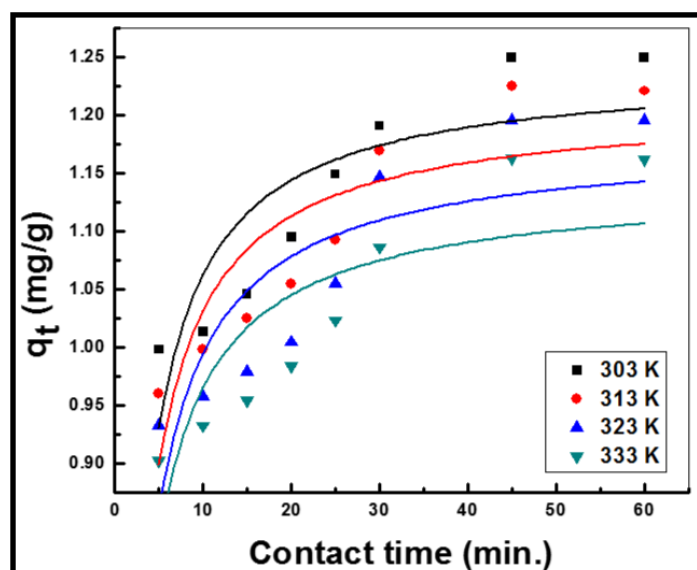


Figure 7.23 Non-linear pseudo-second order plot of chromium removal on nano-cupric oxide obtained by customized Microcal origin function (symbols represent the experimental data and lines represent the data estimated by the model)

Table 7.9 Pseudo-first order and pseudo-second order kinetic parameters for linear analysis and non-linear analysis by customized Microcal origin for adsorption of chromium from aqueous solution on nano-cupric oxide

Analysis	Customized						
	Kinetic model	Pseudo-first order Parameter				Pseudo-second order Parameter	
Temperature (K)	q _e (exp.)	q _e (mg/g)	k ₁ (1/min)	R ² adj.	q _e (mg/g)	k ₁ (1/min)	R ² adj.
303	1.25	1.15	0.35	0.241	0.49	1.24	0.679
313	1.22	1.12	0.34	0.269	0.48	1.21	0.682
323	1.19	1.09	0.33	0.195	0.46	0.46	0.609
333	1.16	1.06	0.34	0.219	0.49	0.49	0.637

7.2.4.3 Intra-particle diffusion

The adsorption data was also fitted to the intra-particle diffusion model for investigating any possibility of diffusion, which is based on diffusive mass transfer where the adsorption rate has been expressed in terms of the square root of time (t) [Weber and Morris, 1963]:

$$q_t = K_{id} t^{0.5} + C \quad (7.11)$$

The plot of q_t vs. the square root of time at different temperatures has been shown in Figure 7.24a. The values of intra-particle diffusion rate constant, K_{id} ($\text{mg g}^{-1} \text{min}^{-1/2}$) and

film thickness, C (mg g^{-1}) calculated from the intercept and slope of the plot, respectively along with their correlation coefficients have been presented in Table 7.10. The slope of the plot represents a rate parameter which is the characteristic of the rate of adsorption in the region where intra-particle diffusion is rate controlling. The constant C is related to the boundary layer thickness; the larger the value of C , the greater will be the boundary layer effect on the adsorption process.

The intra-particle diffusion plot has been demarcated into three regions being marked as 1, 2 and 3 where each domain has its own significance. The regions 1 and 2 have been designated as film diffusion and intra-particle diffusion respectively, whereas region 3 represented the interior surface of adsorbent where adsorption occurred.

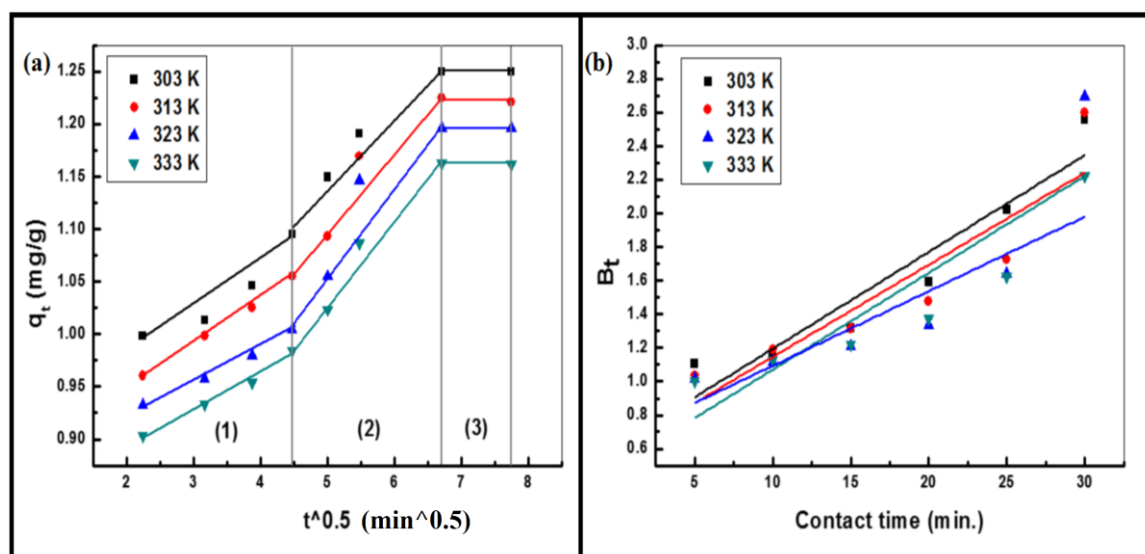


Figure 7.24 (a) Intra-particle diffusion plot for removal of chromium from aqueous solution on nano-cupric oxide. (b) Boyd model plot for removal of chromium from aqueous solution on nano-cupric oxide

In order to be the rate controlling step of the adsorption process, the plots of intra-particle diffusion must pass through the origin. In present case it was observed that it contains multi-linear plots that didn't passed through the origin. This deviation of straight lines from origin may be due to difference in rate of mass transfer in the initial and final stages of adsorption and it indicated that pore-diffusion is not the sole rate-controlling step. It then affirmed that boundary layer diffusion was a rate limiting mechanism for the adsorption of chromium on nano-cupric oxide [Mohanty et al., 2005; Stankovic' et al., 2016].

Table 7.10 Intra-particle diffusion constant values for removal of chromium from aqueous solution on nano-cupric oxide

S. No.	Concentration (mg/L)	K_{id} (mg/g min ^{1/2})	C (mg/L)	R ²
1	303	0.86	0.05	0.930
2	313	0.84	0.05	0.930
3	323	0.78	0.06	0.904
4	333	0.76	0.05	0.939

7.2.4.4 Boyd model

In order to explore the probable mechanism of adsorption further, the Boyd model was applied on the kinetic data. This model distinguishes the film diffusion (boundary

layer) and pore diffusion (diffusion inside adsorbent pores). It can be expressed in the following form [Hu et al., 2011]:

$$B_t = -0.4977 - \ln(1 - F) \quad (7.12)$$

where, F is the fraction of adsorbed adsorbate at any time t (min). B_t was plotted against t and in the present case, the line (Figure 7.24b) did not pass through origin. It indicated that adsorption has been governed by boundary layer diffusion mechanism.

7.2.5 Adsorption thermodynamic study

7.2.5.1 Effect of temperature

The influence of temperature on the removal of Cr(VI) has been investigated at different temperature ranging from 303 to 333 K and at various concentrations pre-defined for the experimentation. It was perceived from Figure 7.25 that percent removal decreases with the temperature and this trend advocated the exothermic nature of the adsorption process. This decrease in percentage of adsorption with increase in temperature may be due to desorption caused by an increase in the available thermal energy that weakened the bonding between heavy metals and active sites [Hua et al., 2011; Pandey et al., 2010]. Increased temperature of the system is supposed to induce higher mobility of the adsorbate leading to desorption and hence the present system is exothermic in nature.

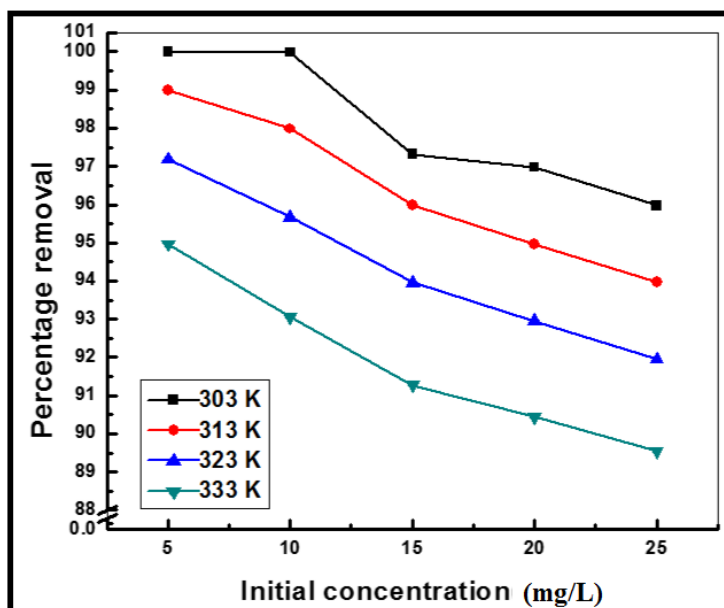


Figure 7.25 Effect of temperature on removal of chromium from aqueous solutions on nano-cupric oxide

7.2.5.2 Thermodynamic parameters

The feasibility and spontaneity of the process was explored by the study of thermodynamic parameters such as changes in standard free energy (ΔG°), enthalpy (ΔH°), and entropy (ΔS°) and were evaluated from Langmuir adsorption model. The following equations have been used for estimation of thermodynamic parameters [Salvestrini et al., 2014; Brown et al., 2009; Elkady et al., 2011]:

$$\Delta G^\circ = -RT \ln K_L \quad (7.13)$$

$$\ln K_L = \Delta S^\circ/R - \Delta H^\circ/RT \quad (7.14)$$

where, ΔG° is the Gibbs free energy change, Langmuir constant b is considered as thermodynamic equilibrium constant; K_L ($L \text{ mol}^{-1}$), R is universal gas constant ($8.314 \text{ J}\cdot\text{mol}^{-1}\cdot\text{K}^{-1}$), and T is the absolute temperature in Kelvin. Subsequently, the values of ΔH° and ΔS° were also determined from the slope and intercept of the plot of $\ln K_L$ vs. $1/T$, respectively. The values of ΔG° , ΔH° and ΔS° calculated at different temperatures have been tabulated in Table 7.11.

The negative ΔG° values affirm feasibility of the adsorption process as well as the spontaneous nature of adsorption that do not require any external source of energy for its occurrence. Further, the decrement in negative value at higher temperature manifested that the spontaneity of adsorption process decline with rise in temperature. In case of physical adsorption, the change of standard free energy varies in the range of -20 to 0 kJ mol^{-1} while for involvement of chemi-sorption standard free energy varies in the range -80 and -400 kJ mol^{-1} [Avila et al., 2014]. Furthermore, the (ΔH°) values were also found to be very low and positive ($1.55 \times 10^{-03} \text{ kJ mol}^{-1}$) which indicated the physical adsorption of Cr(VI) on nano-cupric oxide which was also evident from various characterizations after adsorption besides exhibiting endothermic nature [Sharma et al., 2010]. The positive value of entropy (ΔS°), $586 \text{ J mol}^{-1} \text{ K}^{-1}$ suggested good affinity of Cr(VI) towards the nanoparticles and showed increased randomness at the solid/solution interface during the adsorption process [Saha et al., 2011].

Table 7.11 Thermodynamic parameters for adsorption of chromium from aqueous solution on nano-cupric oxide

S. No.	Temperature (K)	ΔG° (kJ mol ⁻¹)	ΔH° (kJ mol ⁻¹)	ΔS° (J mol ⁻¹ K ⁻¹)
1	303	-34.68	-1.55E-03	586
2	313	-31.27		
3	323	-29.55		
4	333	-24.42		

7.2.5.3 Activation energy

The minimum energy needed for a specific adsorbate-adsorbent interaction to take place during adsorption despite the fact that the process may be thermodynamically feasible is called activation energy. The activation energy (E_a) for the adsorption of an adsorbate ion/molecule onto an adsorbent surface in an adsorption process can be evaluated from the Arrhenius equation as follows [Aksu, 2002]:

$$\ln k_2 = \ln A - E_a/RT \quad (7.15)$$

where, k_2 (g mg⁻¹ min⁻¹) represents the rate constant of pseudo-second order kinetic model, E_a (J mol⁻¹) is the Arrhenius activation energy of adsorption and A is the Arrhenius factor. The values of E_a and A can be obtained from the slope and the intercept

from the plot of $\ln k_2$ versus $1/T$ (Figure 7.26). The activation energy was estimated as 4.26 kJ mol^{-1} .

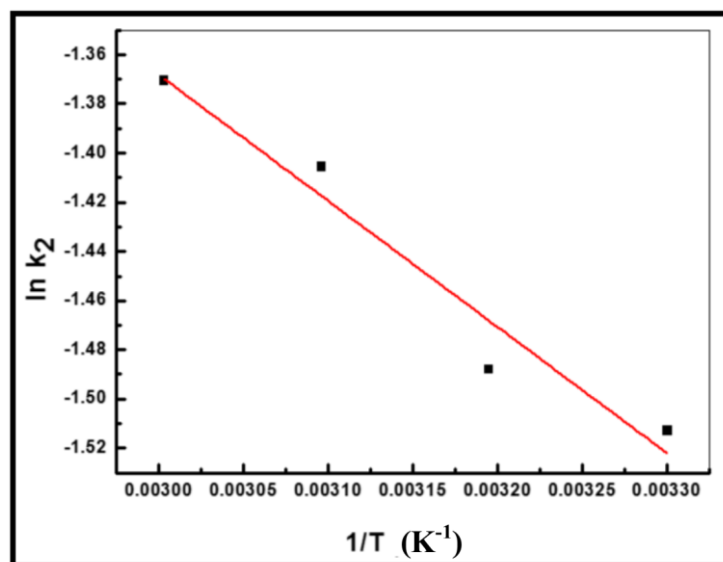


Figure 7.26 Arrhenius plot for removal of chromium from aqueous solution on nano-cupric oxide

7.3 Desorption experiments

The potentiality of exhausted adsorbent for reuse was investigated by conducting desorption experiments with three desorbing agents namely NaOH (Sodium hydroxide), KOH (Potassium hydroxide) and NH_4OH (Ammonium hydroxide). 0.1N of the aforesaid solutions were used to desorb the adsorbed chromium ions from the adsorbent and have shown desorption efficiencies of 99.45 %, 93.29 % and 89.22 % respectively. Among all

the solutions, maximum desorption efficiency has been exhibited by NaOH solution and thus it was selected for the desorption purpose. It was found that up to five consecutive cycles, adsorbent exhibited considerable removal of chromium. After fifth cycle the desorption efficiency was significantly reduced from 98% to 89% (Table 7.9).

Table 7.9 Chromium removal after subsequent regeneration cycle (Initial conc. =10 mg/L, pH = 2.0, Dose = 8g/L, Temperature =303 K)

S. No.	Regeneration cycle	Chromium removal (%)
1	1	98.55
2	2	97.95
3	3	95.37
4	4	93.44
5	5	89.23

7.4 Conclusions

The cupric oxide nanoparticles were successfully explored for removal of Cr(VI) from aqueous solutions. The optimum conditions for achieving the optimum results as predicted by model were initial concentration 5mg/L, pH 2.0 and adsorbent dose 18.84 g/L. However, the results of confirmatory experiments were slightly different from that of

the predictions made by the model. The experimental parameters were optimized for the optimum response. The adsorption equilibrium data was well fitted to Freundlich isotherm model and the kinetics of the adsorption process was well explained through pseudo-second-order kinetic model. The overall process was feasible, spontaneous and exothermic. Linear approach for analysing the isotherm as well as kinetic parameters was found more appropriate than the non-linear approach. The adsorbent was successfully regenerated and reused up to five consecutive cycles without significant loss in removal capacity. The experimental results exhibited that cupric oxide nanoparticles can be a good alternative for Cr(VI) removal from aqueous solutions.